RPE | Radiation Physics & Engineering
A Peer-Reviewed Journal
Published by K.N. Toosi University of Technology
http://rpe.kntu.ac.ir
Research Article

Radiation Physics and Engineering 2026; ?(?):?–?

Thermal properties and dosimetric investigation of Gd_2O_3/ZnO doped glass; Applications in radiation shielding

Imad Hammood Sharqi[a,*], Rihab Zgueb[a], Hassen Dhaouadi[a], Abdelwaheb Boukhachem[b]

[a] *Faculty of Sciences of Tunis, Universit Tunis El-Manar, Tunisia*
[b] *Laboratoire Nanomateriaux et Systemes pour Les Energies Renouvelables (LANSER), Centre de Recherches et des Technologies de L'Energie Technopole Borj Cedria, Tunisia*

HIGHLIGHTS

-
-
-
-
-

ABSTRACT

This study focuses on the ability of both ZnO and Gd_2O_3 used as doping agents in glass in order to replace shielding for lead purposes. The choices of metal-transition oxide and rare earth oxide doping aim to compare shielding results, given their different properties. A thermal study of two series of Zinc oxide and Gadolinium oxide in different percentages is performed. The radiation attenuation properties of these doped glasses were developed. Experimental measurements were performed using a photon spectrometer. Photons incident from Co-60 and Cs-137 sources with main energies of 662, 1173, and 1332 keV were applied to the shield. This study demonstrated that adding either Gadolinium oxide or Zinc oxide to medical glass enhances the radiation attenuation ability, with a preference given to Gadolinium Oxide glass doping. In terms of radiation attenuation, the results obtained with Gadolinium Oxide are comparable to those obtained with lead oxide-doped glass. In addition to the attenuation factors, the thermal properties of each of the mentioned samples were studied under temperature changes.

KEYWORDS

Radiation protection
Doped-Glass
Linear attenuation coefficient
LAC
Photons detector

HISTORY

Received:
Revised:
Accepted:
Published:

1 Introduction

Ionizing radiation can be derived from various sources, industrial and natural (Durante and Cucinotta, 2011). The understanding and characterization of radiation rely on the analysis of its behavior, which is determined by its energy and type (Kohsiek et al., 2007). Radiation is primarily categorized into two main types. The first encompasses bosonic particles and electromagnetic waves, while the second includes massive particles that possess both mass and energy. This group comprises charged particles, such as alpha and beta particles, as well as protons, alongside neutral particles like neutrons (Alcocer and Alcocer, 2021; Kleinknecht, 1998). A fundamental consideration for any location that handles radiation sources, particularly ionizing radiation, is to enhance preventive measures and safety protocols (Part, 2011). Ionizing radiation, particularly gamma rays and X-rays, can significantly harm living cells in the human body, animals and plants through their effects on DNA, leading to disruptions in its molecular structure. Indeed, when cells are exposed to radiation, they can become damaged or die and these damaged or dead cells may lead to cancer or genetic abnormalities. Consequently, while the fundamental principles of protection against ionizing radiation are relatively straightforward to discuss and understand in theory, their practical application presents numerous complexities. By using materials that can shield against radiation, like ceramics, it provides vital safety for workers and the general public in settings and establishments that handle ionizing radiation sources, whether they are industrial, medical, or other facilities that use radiation sources (Tanny, 2015; Gunoglu

*Corresponding author: imadsharqi391@gmail.com

https://doi.org/

and Akkurt, 2021). It is possible to mitigate the impact of radiation doses utilized in various applications. Each category of radiation, determined by its source's intensity and type, necessitates a specific protective strategy tailored to its characteristics. While the primary determinant of reduced radiation exposure is the thickness of the protective material, the type and thickness of this material must also be adapted based on the energy levels and classification of the radiation involved (Osei-Mensah et al., 2012; Waheed et al., 2025). Three fundamental actions can prevent or lessen the harm that ionizing radiation causes, according to the protection from ionizing radiation principle: first, cutting down on exposure duration. Second, increasing as much as possible the distance between the source and the exposed individual, and third, employing protective gear (Oto et al., 2019). These factors are therefore regarded as the essential components of radiation protection, whether direct or indirect. Radiation doses can be absorbed and decreased by utilizing shields made with the proper geometric shapes and dimensions. High-density materials like lead, concrete, and ceramics are generally good at protecting against radiation. Doping glass with ZnO is also used as coming material against (Obaid et al., 2018; Almuqrin et al., 2024).

The selection of appropriate materials to safeguard workers from radiation exposure is a fundamental aspect of radiation protection. This includes the effectiveness of shielding, which is contingent upon the types of materials employed, as these vary according to the radiation type. To increase the density and improve the luminous qualities, doping elements are added to the glass. Gd_2O_3 doped glass exhibits some particular physical and chemical properties that set it apart from other materials through its transparency and lightweight nature (Eevon et al., 2016; Chen et al., 2003). The physical characteristics of glass are altered when doping oxide powder is added. Generally, Gadolinium doped glass composition is affected when exposed to ionizing radiation and this has a significant impact on the resulting materials' characteristics. Additionally, the incorporation of oxide components into its composition enhances its utility across a range of applications, particularly in radiation protection technologies (Al-Buriahi et al., 2025). Several studies have been carried out on the properties of Gadolinium oxide doped glass as a shield against ionizing radiation (Al-Hadeethi et al., 2019; Li et al., 2017). Moreover, it is notable for its diverse applications across multiple sectors, including both biological sciences and contemporary industrial innovations. In industrial settings, gadolinium oxide is employed in conjunction with luminescent networks to enhance the characteristics of specialized sensors and luminescent materials (Sayyed et al., 2025a). Also, Gadolinium oxide is recognized for its chemical stability and thermal stability, exhibiting a low energy threshold of approximately 300-600 cm^{-1}, which can be further improved by the incorporation of lanthanide ions (Hazarika and Mohanta, 2013; He et al., 2017). It is regarded as one of the most valuable composite materials for enhancing the properties of contrast agents in medical imaging, particularly in magnetic resonance and fluorescence applications. This efficacy can be attributed to the valence of gadolinium within the matrix, which facilitates the formation of a highly stable 4f electron shell containing seven unpaired spins, thereby endowing the material with significant magnetization properties (Ansari et al., 2019).

Gadolinium Oxide (Gd_2O_3) exhibits remarkable optical properties, characterized by its ability to absorb specific wavelengths while maintaining transparency. This versatility renders it particularly effective as a shield against gamma rays. This is extremely important, as is the case with CT scans, where professionals such as technicians and physicists working in this field need a clear field of view through the window. Additionally, Gd_2O_3 finds application in various imaging technologies. The optical characteristics of Gadolinium-containing materials can be further enhanced through the doping of these materials with other lanthanide ions. The introduction of activator ions creates opportunities for producing materials that demonstrate significant light transmittance, high Stokes shifts, sharp emission spectra, extended lifetimes, resistance to bleaching, and pronounced photon absorption, thereby functioning as an effective barrier to photons. Furthermore, gadolinium oxide possesses the capability to modulate excitation and emission wavelengths within designated ranges. These unique properties facilitate the use of Gadolinium oxide in a wide range of photonic applications, which include both cutting-edge technological innovations and its use as a shield against radiation (Hazarika and Mohanta, 2013; He et al., 2017). This study seeks to investigate the effect of the incorporation of Gadolinium oxide and Zinc oxide (Gd_2O_3, ZnO) on Na_2O-MgO-Al_2O_3-K_2O-SiO_2-CaO-TiO_2-Fe_2O_3 medical glasses in shielding against gamma rays originating from cobalt and cesium sources across various energy levels. The used doping levels range from 0 to 20% with a step of 5%.

2 Theoretical background

2.1 Linear attenuation coefficient (LAC)

The linear attenuation coefficient serves to elucidate how shielding materials respond to the absorption of photons emitted from radioactive sources. Denoted as (μ), the linear attenuation coefficient quantifies the proportion of photons absorbed by the barrier for each unit of thickness of the absorbing material, with its measurement expressed in units of cm^{-1}. The linear attenuation coefficient is influenced primarily by two factors: the thickness of the shield and the energy of the incident photons (McAlister, 2012). When photons interact with the barrier, Eq. (1) is employed to calculate the number of photons that successfully traverse the material (Johnson, 2017).

$$I = I_0 e^{-\mu x} \tag{1}$$

In this context, I_0 denotes the quantity of photons emitted from the source toward the barrier, while (I) signify the number of photons that successfully penetrate and pass through the barrier. The variable x indicates the thickness of the protective shield employed, and the (μ) symbol represents the attenuation coefficient. In our study,

we utilized Cs-137 sources and Co-60. Figure 1 illustrates the intensity (I_0) of photons emitted by utilized sources, depicted by the red line for Cs-137 and blue line for Co-60 (dashed lines). The solid line represents the photons passing through the barrier as a function of radiation energy with source Cs-137, Co-60.

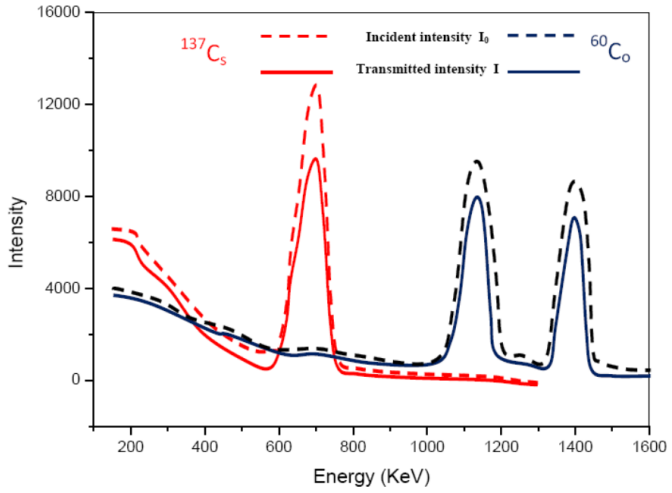

Figure 1: Schematic representation of the incident and transmitted intensity through the barrier versus frequency of radiations originating from sources (Cs-137; Co-60).

2.2 Parameters for photons attenuation

2.2.1 Mean Free Path (MPF)

When radiation penetrates a material, it loses energy through collisions that occur as it moves through the substance. The average distance between these collisions serves as an indicator of the specific interactions taking place. This distance is known as the mean free path, which functions as a protective measure against radiation. Furthermore, the mean free path is inversely related to the material's linear attenuation coefficients (Akkurt et al., 2010).

$$MFP\,(\mathrm{cm}) = \frac{1}{\mu} \tag{2}$$

2.2.2 Half Value Layer (HVL)

The half-value layer (HVL) is a key metric commonly employed to quantify the penetration capability of gamma rays through a given material, representing the distance required for the intensity of radiation to diminish to half of its original value. This measure is typically expressed in centimeters. Consequently, a greater capacity for radiation transmittance corresponds with a higher HVL. The HVL can be calculated using Eq. (3) (Johnson, 2017).

$$HVL = \frac{\ln 2}{\mu} \tag{3}$$

2.2.3 Tenth Value Layer (TVL)

The ability of gamma rays to penetrate a material to a specified depth, referred to as one-tenth of the initial intensity, is termed the tenth-value layer (TVL). The calculation of the TVL is expressed by Eq. (4) (Johnson, 2017).

$$TVL = \frac{\ln 10}{\mu} \tag{4}$$

Calculating the half-value layer (HVL) and tenth-value layer (TVL) values offers significant insights into the capacity of photons to penetrate a radioactive barrier, effectively gauging their penetration probability. These concepts are pivotal in elucidating the design parameters of radiation shielding. The HVL specifically quantifies the material thickness necessary to reduce the intensity of photons emitted from a source to half of their original value, indicating that the intensity of the incident photons is diminished by 50% at this thickness, albeit at varying energy levels. In contrast, the TVL denotes the thickness required to attenuate the radiation to one-tenth of the incident intensity. The mean free path (MFP) serves as a critical and validated parameter in assessing the efficacy of shielding materials in attenuating radiation along its trajectory. The calculations for HVL, TVL, and MFP were derived from the linear attenuation coefficient (LAC), employing Eqs. (2), (3) and (4) for their determination.

3 Experiment

3.1 Samples preparation

Gd_2O_3/ZnO doped medical Glass samples were prepared in the laboratory at Afyon Kocatepe University for Zinc oxide doped-glass, and at the Laboratory of Soft Matter Physics and Fluid Physics (LP2MPF), Faculty of Sciences of Tunis, for Gadolinium oxide doped-glass. Neutral or currently named medical glass had been prepared by melt-quenching technology. The chemical compositions of glasses are displayed in Table 1. Drawing reagent grade Na_2O-MgO-Al_2O_3-K_2O-SiO_2-CaO-TiO_2-Fe_2O_3 as raw materials. In order to achieve its fusion, the mixture powders underwent heat treatment at a temperature of 1200 °C for 20 min. After this process, the prepared sample was placed in an oven at a temperature of 400 °C for 10 h to facilitate gradual cohesion and solidification. Finally, the sample was left to cool naturally at room temperature to the final shape of a disk 20 mm in diameter and 8 mm thickness approximately. Under similar experimental conditions, Gd_2O_3 and ZnO-doped medical glass samples have been fabricated by adding Gd_2O_3 or ZnO to the medical glass powder by keeping a mass of 5gm for each sample. The purity of both Zinc oxide and Gadolinium oxide utilized in this research was 99%. The oxide/glass weight ratios were 0.00, 5%, 10%, 15% and 20%. For the samples designated as (0% ZnO, 0% Gd_2O_3), (Gd_2O_3-5%), (Gd_2O_3-10%), (Gd_2O_3-15%), (Gd_2O_3-20%), (ZnO-5%), (ZnO-10%), (ZnO-15%) and (ZnO-20%) respectively. Each prepared sample was fashioned into a disc measuring 20 mm in diameter and 8 mm in thickness, with each disc weighing 5 grams Fig. 2.

The density of the different samples is measured by the immersion method based on Archimedes' principle according to the following Eq. (5). The liquid used for immersion

Table 1: Chemical Characteristics of the Synthesized Samples (w%).

First doping	Gd_2O_3 0%	Gd_2O_3 5%	ZnO 5%	Gd_2O_3 10%	ZnO 10%	Gd_2O_3 15%	ZnO 15%	Gd_2O_3 20%	ZnO 20%
Second doping	ZnO 0%								
Na2O	14.49	13.77	13.77	13.04	13.04	12.32	12.32	11.59	11.59
MgO	2.31	2.19	2.19	2.08	2.08	1.96	1.96	1.85	1.85
Al_2O_3	2.64	2.51	2.51	2.38	2.38	2.24	2.24	2.11	2.11
K_2O	0.59	0.56	0.56	0.53	0.53	0.5	0.5	0.74	0.74
SiO_2	69.03	65.58	65.58	62.13	62.13	58.68	58.68	55.22	55.22
CaO	10.23	9.72	9.72	9.21	9.21	8.7	8.7	8.18	8.18
TiO_2	0.1	0.1	0.1	0.09	0.09	0.09	0.09	0.08	0.08
Fe_2O_3	0.61	0.58	0.58	0.55	0.55	0.52	0.52	0.49	0.49
Gd_2O_3	0.0	5.0	5.0	10.0	10.0	15.0	15.0	20.0	20.0
ZnO	0.0								

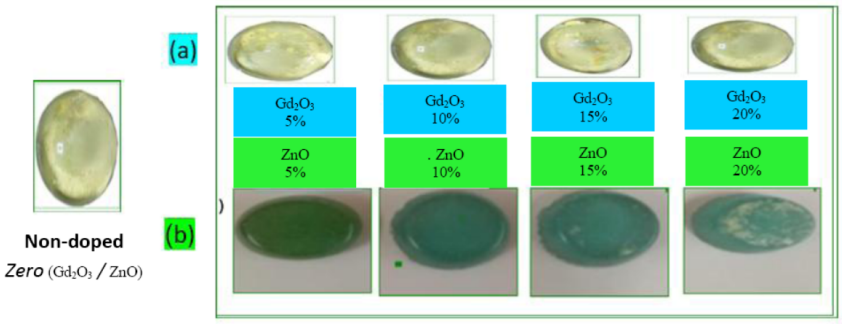

Figure 2: Glass samples doped with Gd_2O_3 (a) and ZnO (b).

is distilled water. The measuring device includes a balance suitable for dry measurement and/or with a sample immersed in water. This device allows a relative accuracy of 0.01 g.cm^{-3} (Rahman et al., 2014).

$$\rho = \rho_0\left(\frac{W_{air}}{W_{air} - W_t}\right) \tag{5}$$

where ρ_0 represents the density of the distilled water, which is 1 g.cm^{-3}. Weir refers to the weight of the glass when it is in air, whereas Wt represents the weight when it is in water. Table 2 shows densities of different doped glass samples used in the experiments. Across various ratios, densities of Gd_2O_3 (respectively ZnO)-doped glass samples vary from 2.745 to 3.482 g.cm^{-3} (respectively from 2.655 to 3.122 g.cm^{-3}). These values are significantly lower than those of lead-doped glasses with densities varying from 3.181 to 4.153 g.cm^{-3} for equivalent percentages (Alsaif et al., 2024). For clarity, the values of the densities in Table 2 are summarized in Fig. 3.

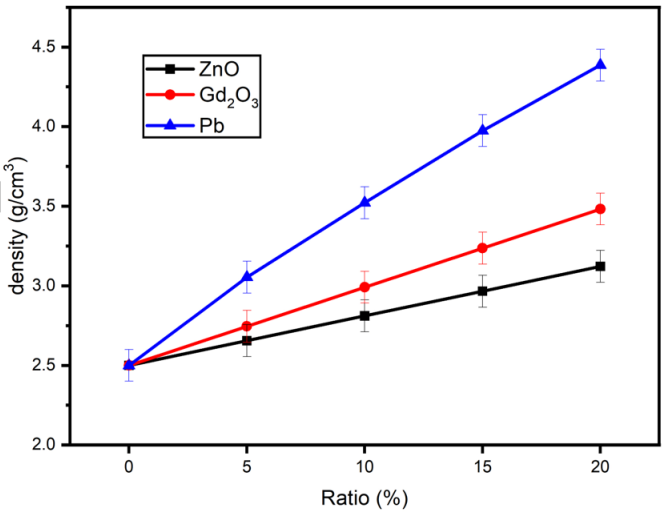

Figure 3: Densities of Pb, ZnO and Gd_2O_3-doped glass samples across various ratios.

3.2 (DSC) measurements

Differential Scanning Calorimetry is a technique of choice for thermal investigations. Easy to use, rapid and reliable, and etc. The principle of this method consists in following and measuring, using thermocouples, the difference in temperatures between the studied sample and one inactive reference body. DSC analyses were carried out during cooling using a specific device, the "Linseis DSC PT 1600", which allows recordings over a wide temperature range from -50 °C to 1400 °C (Azeem et al., 2023).

3.3 (FE-SEM) and (EDX) analysis

The morphology of the sample was studied by utilizing a IGMA variable pressure scanning electron microscope (Fe-SEM). The x-ray spectrometer embedded in the scanning system also provides energy dispersive spectra (EDS) for localized chemical analysis. The EDX mapping was done of some randomly selected regions on the samples.

Figures 4-a and 4-b represent the FE-SEM micrographs; they show the morphology of the samples. Nanoparticles of an average diameter of around 200 nm form

Table 2: Densities of ZnO and Gd_2O_3-doped glass samples across various ratios.

Rate (%)		0	5	10	15	20
Glass density ($g.cm^{-3}$)	ZnO	2.5±0.01	2.655±0.01	2.811±0.01	2.966±0.01	3.122±0.01
	Gd_2O_3	2.5±0.01	2.745±0.01	2.991±0.01	3.236±0.01	3.482±0.01
	Pb_2O	2.5±0.01	3,181±0.01	3,452±0.01	3,875±0.01	4,153±0.01

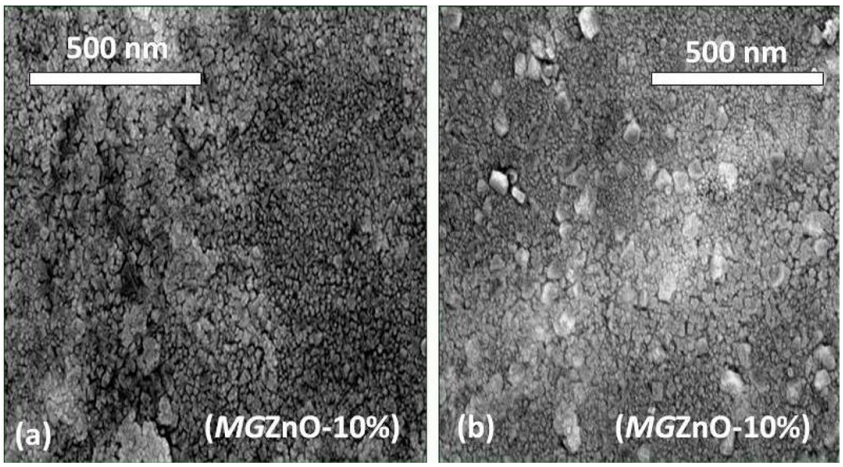

Figure 4: (a) Fe-SEM micrographs for the 10% ZnO-doped-glass, (b) Fe-SEM micrographs for the 10% Gd_2O_3-doped-glass.

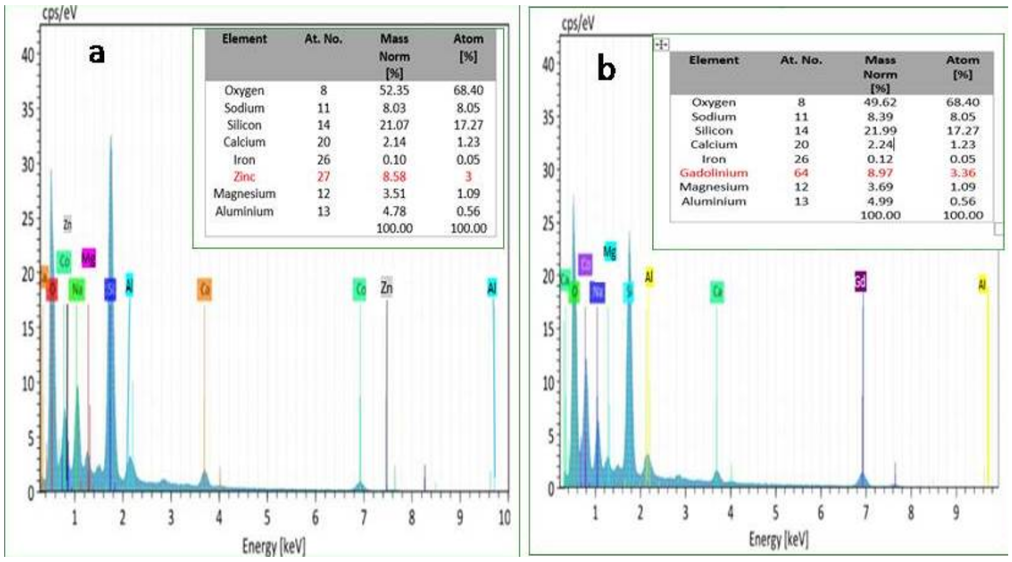

Figure 5: (a) EDX spectra for the (ZnO-10%), (b) EDX spectra (Gd_2O_3-10%).

micrometer-sized aggregates of ZnO/Gd_2O_3-doped-Glass material. The representative EDX spectra, shown in Figs. 5-a and 5-b were collated from a randomly chosen site of the samples, confirming the perfect missibility of all the materials used in the prepared doped glass. A similar conclusion was reported by Azeem et al. in a mixture of Gd_2O_3 doped with Ni, Zn and Fe_2O_4 Nano-particles (Le Losq et al., 2022).

Analysis of selected particles in the mixture shows that the bulk of the particles mainly contains Gd (≈8.97 wt %), oxygen (≈49.62 wt%) and Silicon (≈21.99 wt%) for 10% Gd_2O_3 doped-glass and Zn (≈8.58 wt %), oxygen (≈52.35wt%) and Silicon (≈21.07 wt%) for 10% Gd_2O_3 doped-glass.

3.4 Photons ray Spectrometer

Gamma ray spectroscopy is extensively employed across various disciplines, requires the measurement of ionizing radiation. This technique for assessing ionizing radiation is regarded as a straightforward, non-destructive means of quantifying the photons emitted from a source and detected by an instrument. While a variety of measurement devices are available, each possesses unique technological features. For instance, the NaI(Tl) scintillation detector is notable for its high accuracy and efficiency, while also being relatively cost-effective. An illustrative case of researchers utilizing gamma spectroscopy is that of Alexander Akkurt, who employed a scintillation detector to measure linear attenuation coefficients (Akkurt et al.,

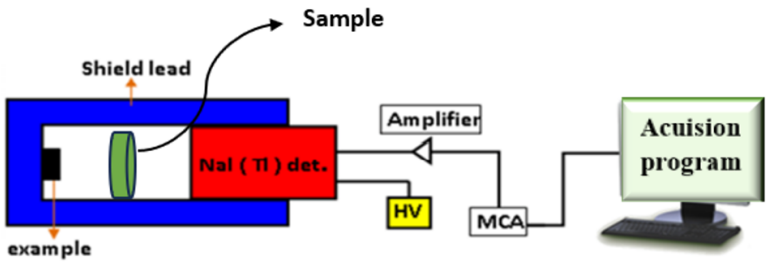

Figure 6: Visual representation of the photon spectrometer and its associated electronic components.

Figure 7: Representation of the NaI(Tl) Detector.

2022). As depicted in Fig. 6, the spectrometer features a schematic layout. The ionizing radiation measurement system comprises a NaI(Tl) scintillation detector with a crystal dimension of 3 inches by 3 inches. Modeling of a $3'' \times 3''$ NaI(Tl) Scintillation Detector System by Monte Carlo Code Program YaynTr: Bildiri / Tam MetinBildiri, Sleyman Demirel niversitesi.

Additionally, Fig. 7 provides an image of the NaI(Tl) detector, which is complemented by an accounting system. The NaI(Tl) detector is a model ORTEC® that consists of several basic components: a $3'' \times 3''$ crystal, a preamplifier, a multichannel analyser with 16384 channels, and a PC to record the data. The signals from the detector were analyzed by MCA using ORTEC® Maestro® software (Akkurt, 2015). The energy resolution of NaI (Tl) detector (6.9% @ 662 keV) and other parameters of the detection system have been described elsewhere (ORTEC, 2020).

This database represents the geometric configuration generated by photons. Typically, we initiate activation of the crystal using a thalidomide activator; this is necessary because the crystal ceases to function as a result of electron transfer. The scintillation detector, comprising a photocathode and a photomultiplier tube (PMT), is employed to detect the emitted photon rays. The detector utilized for this purpose is sodium iodide doped with thallium (NaITl). The process begins with the absorption of a photon by the detector device, which subsequently converts this photon into light, primarily in the near-visible spectrum. The cathode plays a critical role by transforming the incoming photons from the source into an electron beam. Following this conversion, the electrons are intensified by reflective mirror diodes. Once amplified, the resulting pulse is directed to the spectral analysis program for further evaluation (Leo, 1988).

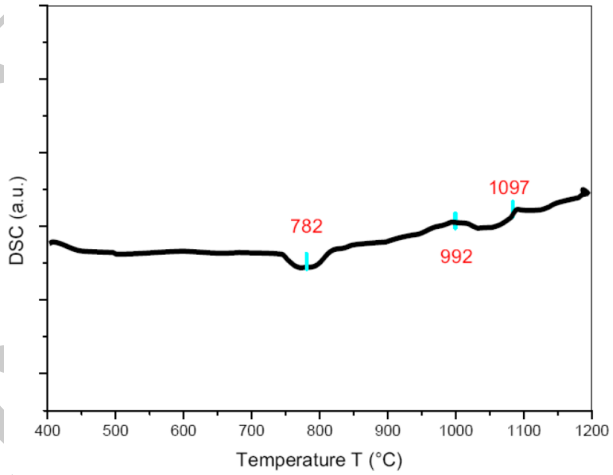

Figure 8: DSC diagram for non-doped medical glass.

4 Results and discussions

4.1 Thermal analysis

(DSC) Differential scanning calorimetry measurements are performed during cooling at a constant gradient of 5 ° per minute. Figure 8 shows the DSC diagram associated with non-doped medical glass. The measurement results are summarized in Fig. 9 for the two series doped with Zinc oxide and Gadolinium oxide. The different curves present several breaks and changes in appearance characteristic of mixtures of several constituents in these samples. The observation of the DSC curves makes it possible to detect the presence of three main phase transitions during cooling for all the samples analyzed. The first is that corresponding to the glass transition. It occurs at a temperature noted T_g. The second corresponds to the appearance of the crystalline phase at the temperature T_c. Finally, the melting takes place at the temperature T_f. Figure 10 represents

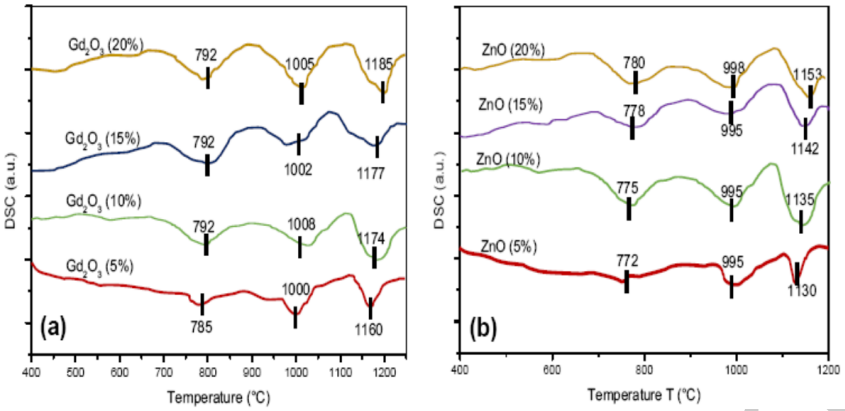

Figure 9: DSC diagrams for series of Gd_2O_3 doped-glass (a) and ZnO doped-glass (b).

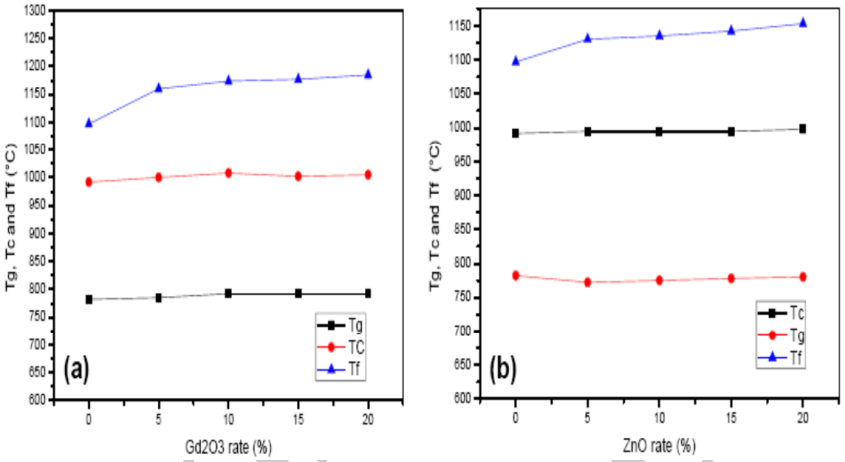

Figure 10: Evolution of the phase transition temperature T_g, T_c and T_f as a function of doping rate for both series Gd_2O_3 doped-glass (a) and ZnO doped-glass (b).

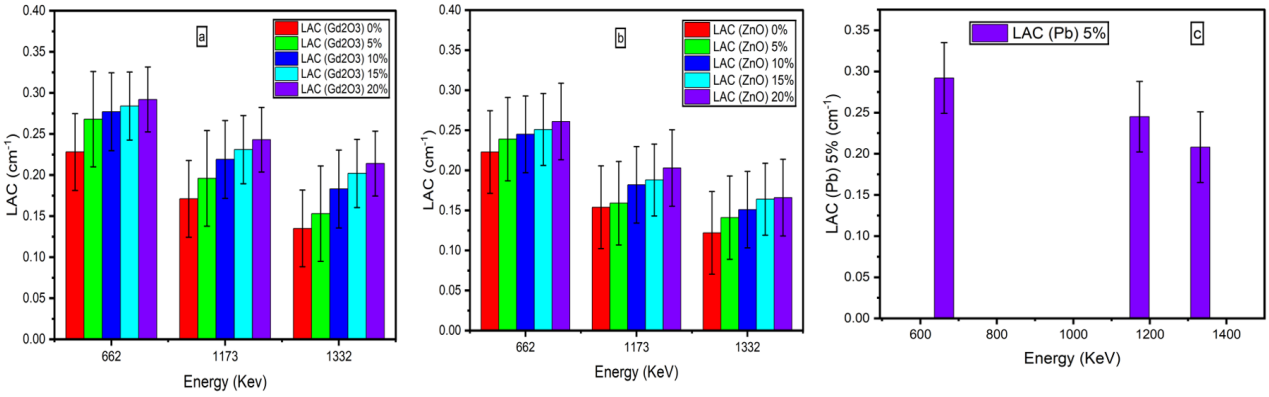

Figure 11: Evolution of the LAC as a function of energy for each doped sample: ZnO (a), Gd_2O_3 (b) And 5% Pb (c).

the evolution of the temperatures T_g, T_c, T_f, as a function of the doping percentage.

The measurement results show a slight change in the phase transition temperatures with doping. This increase is higher for Gadolinium oxide-doped samples than those doped with Zinc oxide. This evolution is particularly expected for samples with high doping, given that the melting temperatures of the doping entities are 2420 ° for Gadolinium oxide and 1975 ° for Zinc oxide (Özgür et al., 2005).

4.2 LAC measurements

The radiation shielding characteristics of the various prepared glass samples have been evaluated, with measurements conducted in accordance with the parameters outlined in Section 3. The linear attenuation coefficients (μ) were derived and are presented as a function of gamma ray energy for each sample type in Fig. 11. Analysis of these figures reveals that the linear attenuation coefficients exhibit a linear decrease as gamma ray energy increases.

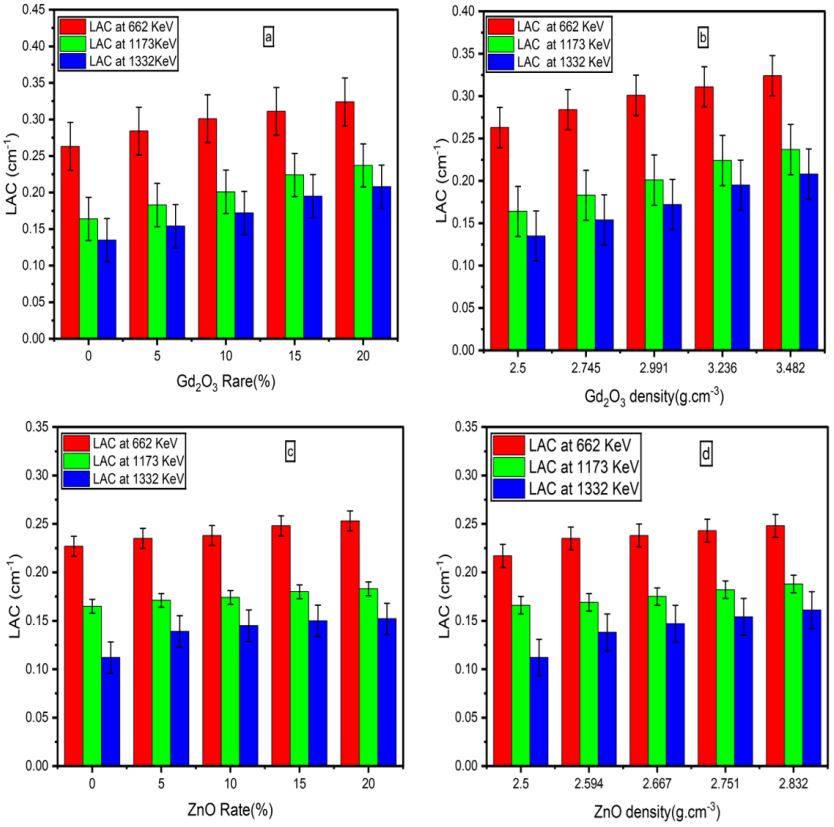

Figure 12: Evolution of the LAC as a function of density and ratio of Gd_2O_3 (a, b) and ZnO (c, d).

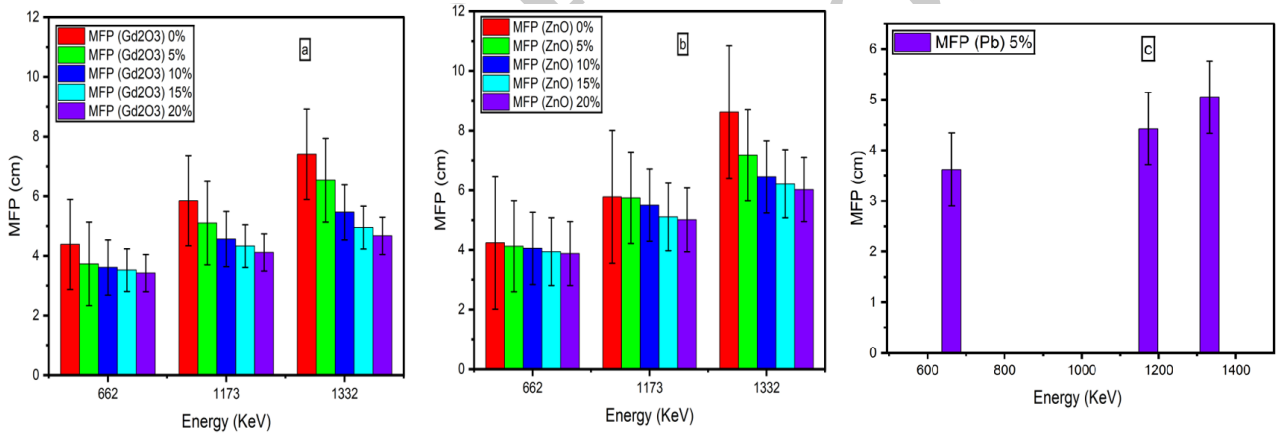

Figure 13: Evolution of the Parameter (MFP) as a function of energy for each sample doped with Gd_2O_3 (a), ZnO (b) and 5% Pb.

By comparing A and form B, the results confirmed that Gd_2O_3, represented by form B, has greater protective capacity than ZnO in form A, which is consistent with the published study (Sayyed et al., 2025b).

In Fig. 12, the LAC in the studied samples is plotted as a function of the doping ratios (a and c) and of the densities (b and d). These diagrams show a superior ability of doping with Gadolinium oxide to attenuate the irradiation doses in all wavelengths used compared to Zinc oxide at equal percentages. The LAC values measured in this study (Gd_2O_3, ZnO) for doped samples are comparable to those reported in the literature for lead-doped glass, where (μ) changes from 0.75 to 7.25 cm^{-1} depending on the doping rate and its nature (Mukamil et al., 2022). Arzu Poyraz et al found values of about 0.32 to 0.42 cm^{-1} in the first mixture A(50% ZrB_2, 50%PbO) and 0.62 cm^{-1} to 0.75 cm^{-1} for the second mixture B(50% ZrB_2. 50%PbO. 10%CuO. 10%ZnO. 30%TiO_2) (Poyraz et al., 2025).

4.3 (MFP), (HVL) and (TVL) measurements

To illustrate the radiation shielding capabilities of glass, additional parameters can be utilized. This includes the mean free path (MFP), half value layer (HVL), and tenth value layer (TVL). The (MFP) data for Zinc oxide, Gadolinium oxide and 5% Pb are shown in Fig. 13, plotted

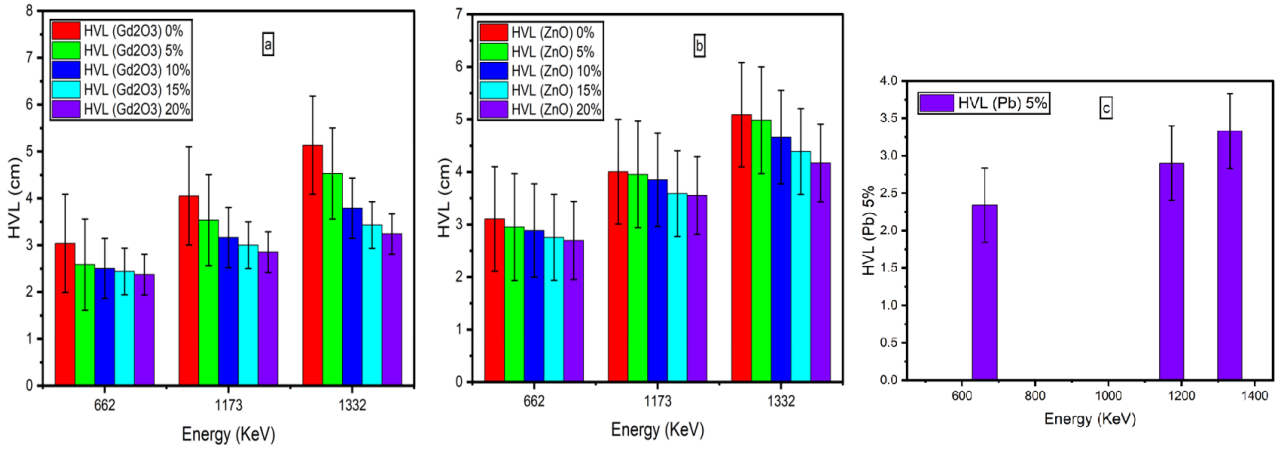

Figure 14: Evolution of the Parameter (hvl) as a function of energy for each sample doped with Gd_2O_3 (a), ZnO (b) and 5% Pb (c).

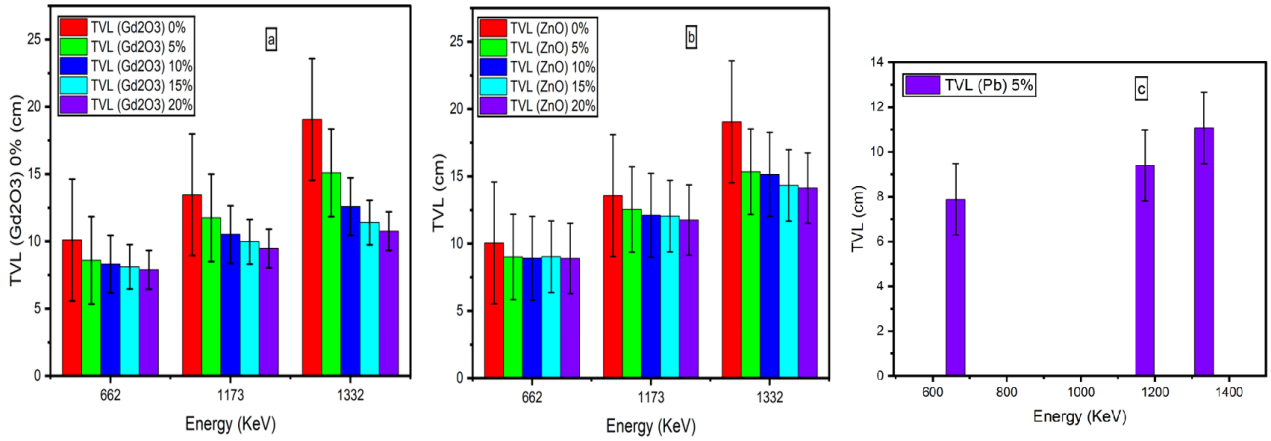

Figure 15: Evolution of the Parameter (TVL) as a function of energy for each samples doped with Gd_2O_3 (a), ZnO (b) and 5% Pb (c).

against gamma ray energy for cesium, and cobalt. These figures demonstrate that the MFP increases with higher gamma ray energy, with a similar trend observed for both entities (Gd_2O_3, ZnO and 5% Pb). This indicates that distance plays an important role in reducing exposure and is necessary to attenuate high-energy gamma rays compared to low-energy ones. The HVL results, depicted in Fig. 14 for various samples as a function of gamma ray energy, further reveal that HVL also rises with increasing gamma ray energy, with cadmium showing a more pronounced advantage (El-Ghany et al., 2020). This implies that a longer material thickness is required to shield high-energy gamma rays effectively. Additionally, Fig. 15 presents the TVL results as a function of photon beam energy across different types of glass. It is evident from these figures that the TVL increases with photon ray energy, suggesting that the material length necessary to attenuation high-energy gamma rays exceeds that needed for low-energy gamma rays. From the results shown in Figs. 14 and 15, we note that increasing the different weight ratios led to enhancing the concentration of impurities and thus directly reducing the HVL and TVL values. This is entirely consistent with the published results (Mehrara et al., 2021).

5 Conclusions

Since radiation is a part of our daily lives, particularly with the advancement of technology, it is crucial to be mindful of the potentially harmful consequences that radiation may have on cells. This requires creating new and lead-alternative materials. study, doped glass with Gadolinium oxide and Zink oxide (Gd_2O_3, ZnO) was chosen for investigation against gamma rays originating from cobalt and cesium sources across various energy levels of gamma rays (662, 1173, and 1332 keV), which were created using Co-60 and Cs-137 sources. The aim of this study is to compare the effect of adding these oxides to medical glass on the attenuation of ionizing radiation and to compare the test results with previous similar studies. In addition to the effect on the radiation shielding properties, doping glasses with ZnO and Gd_2O_3 had an important effect on the thermal characteristics. Phase transition temperatures undergo a slight increase with doping. This increase is higher for Gadolinium oxide-doped samples than for Zinc oxide-doped samples. This slight increase does not represent an obstacle to the use of doped glass as a radiation attenuator, as glass manufacturing methods can

ignore this increase without additional cost.

Several parameters have been examined in this study regarding our prepared samples. LAC, HVL, and MFP are calculated for two series (0%, 5%, 10%, 15%, and 20%) of doped glass. The first is doped with zinc oxide (ZnO), and gadolinium oxide (Gd_2O_3) for the second one. From the measured results, it was observed that the linear attenuation coefficient decreases with the increasing energy of the incident gamma rays. On the other hand, it was clearly seen.

With increasing zinc oxide concentration on the glasses, the linear attenuation coefficient increased linearly. The results confirm those found in the literature for different types of doping and mixtures. These results enabled us to compare the efficiency of both additives to the glass. Tests showed that gadolinium oxide had a better effect on the attenuation process with a slight difference in density. It also provided better transparency while maintaining a clear, uncolored glass, as is the case with zinc oxide. In conclusion, we can talk about Gadolinium oxide as an alternative to lead as an additive to glass, as it provides better transparency and a good ability to attenuate ionizing radiation without an enormous increase in its density.

Conflict of Interest

The authors declare no potential conflict of interest regarding the publication of this work.

Funding

The authors declare that no funds, grants, or other financial support were received during the preparation of this manuscript.

References

Akkurt, I. (2015). Variation of energy resolution with distance for a NaI (Tl) detector. *Acta Physica Polonica A*.

Akkurt, I., Akyıldırım, H., Mavi, B., et al. (2010). Photon attenuation coefficients of concrete includes barite in different rate. *Annals of Nuclear Energy*, 37(7):910–914.

Akkurt, İ., Waheed, F., Akyildirim, H., et al. (2022). Performance of NaI (Tl) detector for gamma-ray spectroscopy. *Indian Journal of Physics*, 96(10):2941–2947.

Al-Buriahi, M., Echeweozo, E., Sriwunkum, C., et al. (2025). Gamma radiation shielding and interaction properties of MoO3-Doped cadmium zinc lithium-borate glasses. *Nuclear Engineering and Technology*, 57(4):103313.

Al-Hadeethi, Y., Sayyed, M., Kaewkhao, J., et al. (2019). An extensive investigation of physical, optical and radiation shielding properties for borate glasses modified with gadolinium oxide. *Applied Physics A*, 125(11):749.

Alcocer, G. and Alcocer, P. (2021). Burns by ionizing and non-ionizing radiation. *Mediterranean Journal of Basic and Applied Science*, 5(1):86–103.

Almuqrin, A. H., Sayyed, M., Kumar, A., et al. (2024). Characterization of glasses composed of PbO, ZnO, MgO, and B_2O_3 in terms of their structural, optical, and gamma ray shielding properties. *Nuclear Engineering and Technology*, 56(7):2842–2849.

Alsaif, N. A., Alfryyan, N., Al-Ghamdi, H., et al. (2024). Optical and gamma-ray attenuation of cobalt and lanthanum-doped sodium zinc lead borate glass. *Journal of Materials Science: Materials in Electronics*, 35(21):1458.

Ansari, A. A., Ahmad, N., and Labis, J. P. (2019). Highly colloidal luminescent porous tb-doped gadolinium oxide nanoparticles: Photophysical and luminescent properties. *Journal of Photochemistry and Photobiology A: Chemistry*, 371:10–16.

Azeem, M., Abbas, Q., Abdelkareem, M., et al. (2023). Band gap and pseudocapacitance of Gd2O3 doped with Ni0. 5Zn0. 5Fe2O4. *Physica Scripta*, 98(1):015838.

Chen, Q., Ferraris, M., Milanese, D., et al. (2003). Novel Er-doped PbO and B_2O_3 based glasses: investigation of quantum efficiency and non-radiative transition probability for 1.5 μm broadband emission fluorescence. *Journal of Non-crystalline Solids*, 324(1-2):12–20.

Durante, M. and Cucinotta, F. A. (2011). Physical basis of radiation protection in space travel. *Reviews of modern physics*, 83(4):1245–1281.

Eevon, C., Halimah, M., Zakaria, A., et al. (2016). Linear and nonlinear optical properties of Gd3+ doped zinc borotellurite glasses for all-optical switching applications. *Results in Physics*, 6:761–766.

El-Ghany, S. A., Nabhan, E., and Saudi, H. (2020). Effect of gamma ray on some properties of bismuth borate glasses containing different transition metals. *SN Applied Sciences*, 2(5):832.

Gunoglu, K. and Akkurt, İ. (2021). Radiation shielding properties of concrete containing magnetite. *Progress in Nuclear Energy*, 137:103776.

Hazarika, S. and Mohanta, D. (2013). Production and optoelectronic response of Tb3+ activated gadolinium oxide nanocrystalline phosphors. *The European Physical Journal-Applied Physics*, 62(3):30401.

He, S., Zhao, X., and Tan, M. C. (2017). Synthesis of uniform rare earth doped Gd_2O_2S sub-micron sized spheres using gas-aided sulfurization and their optical characteristics. *RSC Advances*, 7(57):35738–35751.

Johnson, T. E. (2017). *Introduction to health physics*. McGraw Hill Professional.

Kleinknecht, K. (1998). *Detectors for particle radiation*. Cambridge University Press.

Kohsiek, W., Liebethal, C., Foken, T., et al. (2007). The Energy Balance Experiment EBEX-2000. Part III: Behaviour and quality of the radiation measurements. *Boundary-Layer Meteorology*, 123(1):55–75.

Le Losq, C., Tarrago, M., Blanc, W., et al. (2022). Méthodes d'analyse des verres. *Matériaux & Techniques*, 110(4):403.

Leo, W. R. (1988). Techniques for nuclear and particle physics experiments. *Nucl Instrum Methods Phys Res*, 834:290.

Li, R., Gu, Y., Wang, Y., et al. (2017). Effect of particle size on gamma radiation shielding property of gadolinium oxide dispersed epoxy resin matrix composite. *Materials Research Express*, 4(3):035035.

McAlister, D. R. (2012). Gamma ray attenuation properties of common shielding materials. *University Lane Lisle, USA*.

Mehrara, R., Malekie, S., Kotahi, S. M. S., et al. (2021). Introducing a novel low energy gamma ray shield utilizing Polycarbonate Bismuth Oxide composite. *Scientific Reports*, 11(1):10614.

Mukamil, S., Ullah, I., Sarumaha, C., et al. (2022). Lead-borate glass system doped with Sm3+ ions for the X-ray shielding applications. *Results in Physics*, 43:106121.

Obaid, S. S., Gaikwad, D. K., and Pawar, P. P. (2018). Determination of gamma ray shielding parameters of rocks and concrete. *Radiation Physics and Chemistry*, 144:356–360.

ORTEC (2020). High-Resolution Gamma-Ray Spectroscopy. ORTEC Experiment 3. Gamma-Ray Spectroscopy Using NaI(Tl) Equipment Required. Purpose. Gamma Emission. *ORTEC Experiment 3*.

Osei-Mensah, W., Fletcher, J. J., and Danso, K. A. (2012). Assessment of radiation shielding properties of polyester steel composite using MCNP5. *International Journal of Science and Technology*, 2(7):231–236.

Oto, B., Kavaz, E., Durak, H., et al. (2019). Effect of addition of molybdenum on photon and fast neutron radiation shielding properties in ceramics. *Ceramics International*, 45(17):23681–23689.

Özgür, Ü., Alivov, Y. I., Liu, C., et al. (2005). A comprehensive review of ZnO materials and devices. *Journal of Applied Physics*, 98(4).

Part, N. (2011). Radiation protection and safety of radiation sources International Basic Safety Standards. *Interim Edition*.

Poyraz, A., Yigitoglu, I., Canimkurbey, B., et al. (2025). Experimental and theoretical investigation of gamma radiation absorption properties of oxide nanoparticles. *Journal of Materials Science: Materials in Electronics*, 36(10):634.

Rahman, A., Singh, A., Karumuri, S., et al. (2014). Graphene reinforced silicon carbide nanocomposites: processing and properties. In *Composite, Hybrid, and Multifunctional Materials, Volume 4: Proceedings of the 2014 Annual Conference on Experimental and Applied Mechanics*, pages 165–176. Springer.

Sayyed, M., Mahmoud, K., and Hanafy, T. A. (2025a). A new protective glass material against gamma ray: Thorough analysis to determine the impact of adding gadolinium (III) oxide. *Nuclear Engineering and Technology*, 57(1):103146.

Sayyed, M., More, C. V., Hanfi, M. Y., et al. (2025b). Impact of BaO on the gamma-ray shielding performance of lanthanum barium-borate glasses. *Scientific Reports*, 15(1):37009.

Tanny, S. M. (2015). *Investigation of radiation protection methodologies for radiation therapy shielding using Monte Carlo simulation and measurement*. PhD thesis, University of Toledo.

Waheed, F., Al-Sudani, M. A. M., and Akkurt, I. (2025). The experimental enhancing of the radiation shield properties of some produced compounds. *International Journal of Applied Sciences and Radiation Research*, 2(1).

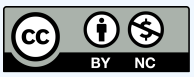

To cite this article:

I. H. Sharqi, R. Zgueb, H. Dhaouadi, A. Boukhachem. Thermal properties and dosimetric investigation of Gd_2O_3/ZnO doped glass; Applications in radiation shielding. *Radiation Physics and Engineering*, In Press.

DOI:

To link to this article: